SAMPLING OF BUILDING SURFACES TOWARDS AN EARLY ASSESSMENT OF BIPV POTENTIAL IN URBAN CONTEXTS

Giuseppe Peronato	Ecole polytechnique fédérale de Lausanne (EPFL) | LIPID	giuseppe.peronato@epfl.ch
Emmanuel Rey	EPFL | LAST	emmanuel.rey@epfl.ch
Marilyne Andersen	EPFL | LIPID	marilyne.andersen@epfl.ch

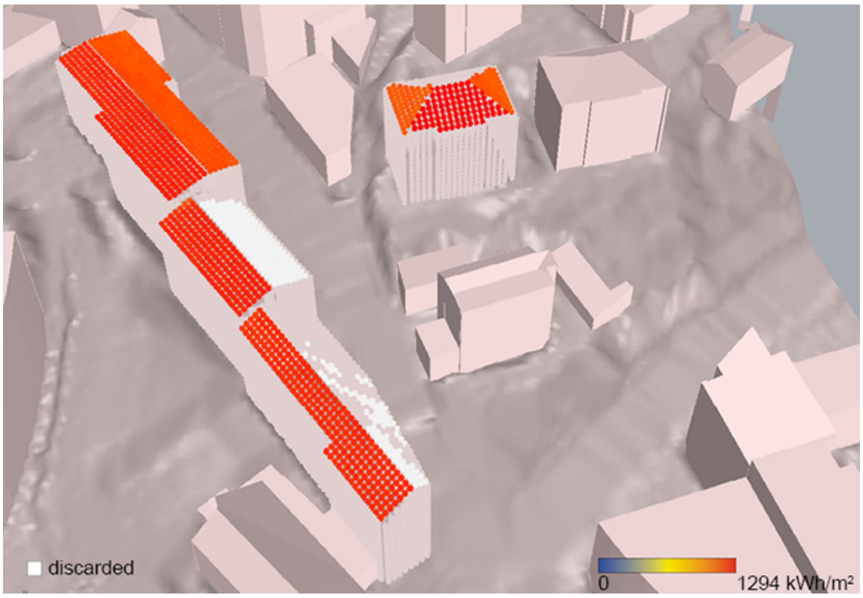

Fig 1: BIPV-suitable surfaces as defined by the proposed algorithm (conservative approach, threshold = 975 kWh/m^2)

WHICH ARE YOUR ARCHITECTURAL (R)SOLUTIONS TO THE SOCIAL, ENVIRONMENTAL AND ECONOMIC CHALLENGES OF TODAY?

Research summary

Although the integration of PV systems in the building envelope (BIPV) is an important factor for the acceptability of such installations, current urban-scale solar potential metrics only partially consider this aspect. As part of the definition of BIPV-suitable surfaces, we argue that a geometric-regularity criterion can help predict the possible disposition of solar panels already in the early assessment of BIPV potential in urban contexts.

To address this need, we developed an algorithm for the geometric sampling of the parts of the building envelope achieving a minimum irradiation threshold, with the aim of defining uniformly-covered active solar surfaces. The proposed methodology is implemented in a flexible parametric design platform and tested in a case study in Neuchâtel (Switzerland). We show that integrating geometric regularity in the assessment of BIPV potential can have a significant influence in the calculation of the solar energy production and discuss the value of such information in urban planning practices.

Keywords: building-integrated photovoltaics (BIPV), solar potential, sustainable urban planning

1. Introduction

With the "Energy Strategy 2050" (SFOE, 2014), Switzerland is planning to gradually withdraw from the use of nuclear energy and consequently integrate a larger share of renewable energy sources. On the basis of the estimated photovoltaic (PV) potential on building surfaces (IEA, 2002), it can be calculated that the solar power production could cover 29.6% of the current electricity consumption of Switzerland (SFOE, 2015). However, despite the continuous advancements in solar cell technologies and the reduction of fabrication costs, the large-scale implementation of photovoltaics as an integrated part of the building envelope (BIPV) encounters several obstacles, such as the lack of a holistic approach starting from the planning phase (Heinstein, Ballif, & Perret-Aebi, 2013).
Different methods exist for calculating the active solar potential of the urban fabric on both roofs and facades, using either CAD- (Compagnon, 2004; Kanters, Wall, & Dubois, 2014) or LiDAR-based 3D models (Jakubiec & Reinhart, 2012; Redweik, Catita, & Brito, 2013). In all of them, the PV-suitability of building surfaces is calculated by the achievement of a minimum solar irradiation threshold, usually defined by the payback time (Jakubiec & Reinhart, 2012; Kanters et al., 2014). However, little attention is given to the effective integration of solar systems in the urban envelope in terms of visual appearance, although this is an important factor for the urban acceptability of such installations and – for the case of Switzerland – to get public subsidies (Munari Probst & Roecker, 2011).
Among all integration criteria, the architectural quality of the intervention is particularly difficult to evaluate before the system being actually designed, e.g. during an urban-scale assessment. However, we argue that a regular geometric disposition of PV-suitable surfaces, which is generally not considered in irradiation maps, is a prerequisite for the coherence of the PV installation with the "global building design logic" (Munari Probst & Roecker, 2011) and for its alignment to the existing building elements (SMS, 2013).
This paper thus presents a sampling algorithm with the goal of introducing a geometric-regularity criterion since the early assessment of BIPV potential in urban contexts. Two approaches towards geometric regularity are evaluated and compared with a standard calculation method based only on a solar irradiation threshold. This algorithm is implemented into a parametric design platform, coupled with a solar radiation simulation tool, and tested in a CAD-based urban 3D model automatically-reconstructed from LiDAR data. We show that the proposed approaches can have a significant influence in the calculation of the solar energy production. We argue that such difference should be taken into account by planners and decision-makers while calculating the solar energy potential at the urban scale.

2. Methodology

The proposed methodology integrates a geometry-sampling algorithm and an evaluation of the BIPV-suitability of building surfaces in order to predict the possible installation of BIPV systems.

2.1 Geometry sampling

The sampling algorithm is based on a geometric-regularity criterion. Its definition is inspired by a selection of design guidelines provided by SMS (2013), such as "regrouping the [PV] elements", "adopting preferably a rectangular shape" and "respecting building contours and the parallelism of lines" (translation ours). Two approaches, both aiming at geometric regularity in the disposition of solar panels, but opposed in terms of the use of the solar irradiation threshold as a decision criterion, are proposed here. In the former, which we refer to as the conservative approach, the parts of the facade that, despite achieving the irradiation threshold, prevent a regular disposition of solar panels on that surface are discarded. Conversely, the aggressive approach takes into account also those parts of the facade that, despite not achieving the irradiation threshold, allow a regular disposition of solar cells on that surface.

This concept is implemented in an algorithm that analyzes the grid of points created on each building surface to be used as sensors in the simulation of solar radiation. These points are organized in parallel horizontal lines, as shown in Fig 2, so that their belonging to a particular line can be used in the sampling algorithm to determine if the geometric-regularity objective is fulfilled. In the conservative approach, a sensor $p_{b,s,l}$ is considered suitable for BIPV installation only if all the sensors on the line $l_{b,s}$ achieve the irradiation threshold. Conversely, in the aggressive approach, if a certain number (n_{min}) of sensor points $p_{b,s,l}$ of the line $l_{b,s}$ achieve the irradiation threshold, all the sensor points on the line $l_{b,s}$ are considered suitable for a BIPV installation. As can be seen in Fig 2, by using the aggressive approach, two points not achieving the threshold are considered acceptable. The minimum number of sensor points (n_{min}) for a line to be considered suitable can be freely fixed by the user. The smaller its value is, the greater is possibly the number of sensor points that will be considered suitable despite not achieving the irradiation threshold. In this paper, the most extreme scenario, i.e. $n_{min} = 1$, was chosen in order to show the maximum possible increment in energy production that can be obtained by this approach. However, if the choice of the irradiation threshold is determined by an economic or environmental minimum payback time, the decision-maker should accept the risk of the non-viability of the installation. If such viability is determinant for the project and the geometric regularity is still considered an important factor, the conservative approach should be chosen instead.

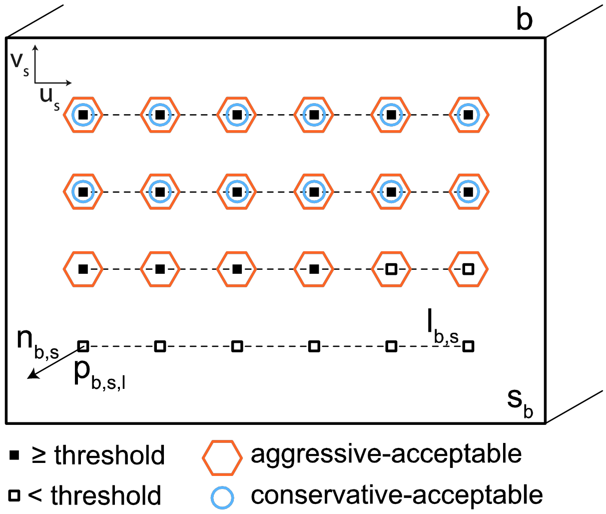

Fig 2: Definition of sensor points and of the geometric-acceptability approaches

2.2 PV systems and building surfaces

All sensor points $p_{b,s,l}$ are coupled with a vector representing the normal $n_{b,s}$ to the surface s they belong to (Fig 2). This vector can be used to identify the inclination of the surface s over the horizontal plane. Since the tilt angle influences the direct radiation arriving at an inclined surface (Häberlin, 2012, para. 2.5.3.1) as well as the possible PV-mounting systems, we argue that such information can help assign to each building surface the most appropriate PV panel (e.g. tilted panels on flat roofs, envelope-integrated panels on sloped and vertical opaque surfaces) and solar cell technology (e.g. crystalline-silicon modules on roofs, thin-films on facades). This choice can be finally supported by additional analyses (not included in this work), such as the exposition or the number of sunlight hours.

3. Case-study application

The proposed algorithm is implemented in a case study in the city of Neuchâtel (Switzerland) following the workflow described in Fig 6 and in the following paragraphs. The three buildings selected for this study (Fig 3) are considered representative of some common building typologies in Swiss urban areas and present relevant characteristics for the purpose of this study.

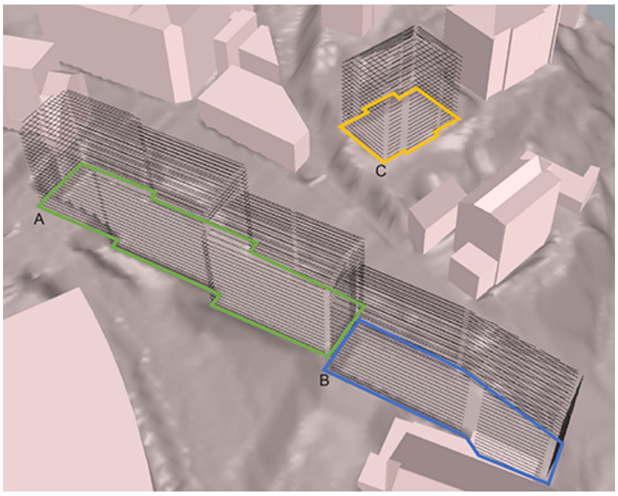

Fig 3: Definition of lines on building surfaces; in color, the footprint of the three simulated buildings

Buildings A and B are two gable-roofed row buildings, whereas building C is a hip-roofed detached building. The inclination of the roofs ranges from 10-20° for building A to about 30° for buildings B and C (Fig 5). They present different orientations, as can be seen in Fig 4. The envelope of buildings A and B are mostly oriented towards East and West, while building C has mainly a North-South orientation. Building C thus presents both the best orientation and roof inclination, reaching the highest irradiation values of 1294 kWh/m^2 (Fig 4 and Fig 5). Finally, one should also note that all buildings are prevalently residential and do not have any photovoltaic panel or solar collector installed yet.

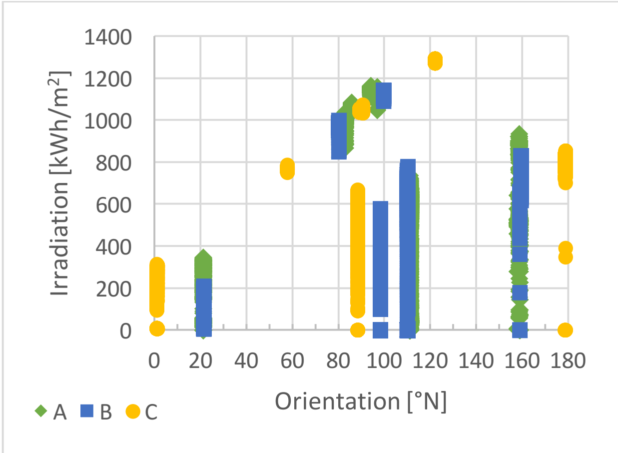

Fig 4: Distribution of sensor points over the orientation and irradiation for buildings A, B and C

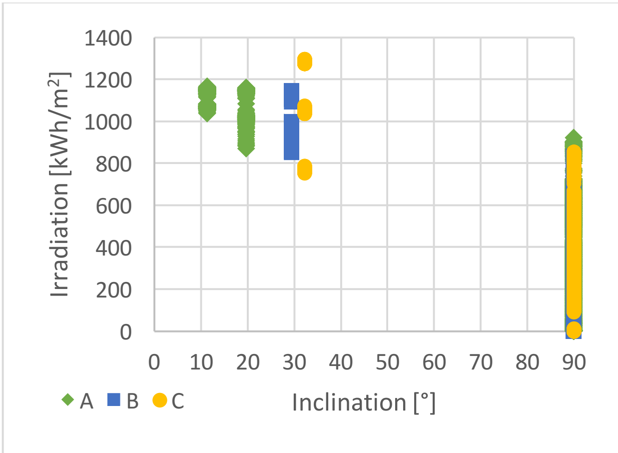

Fig 5: Distribution of sensor points over the inclination and irradiation for buildings A, B and C

3.1 Modeling

The 3D model is created using the software BuildingReconstruction (virtualcitySystems, 2014) on the basis of high-definition GIS data, according to the Level of Detail 2 (LOD2) of the CityGML standard (Kolbe, Gröger, & Plümer, 2005). This modeling workflow is implemented in Grasshopper (McNeel, 2014) through its standard components.

The distance between points, in both u and v directions, was set to 1 m, as it is considered a standard value for urban-scale solar simulations (Compagnon, 2004). However, it is possible to use other values in order to reflect the actual dimension of solar panels.

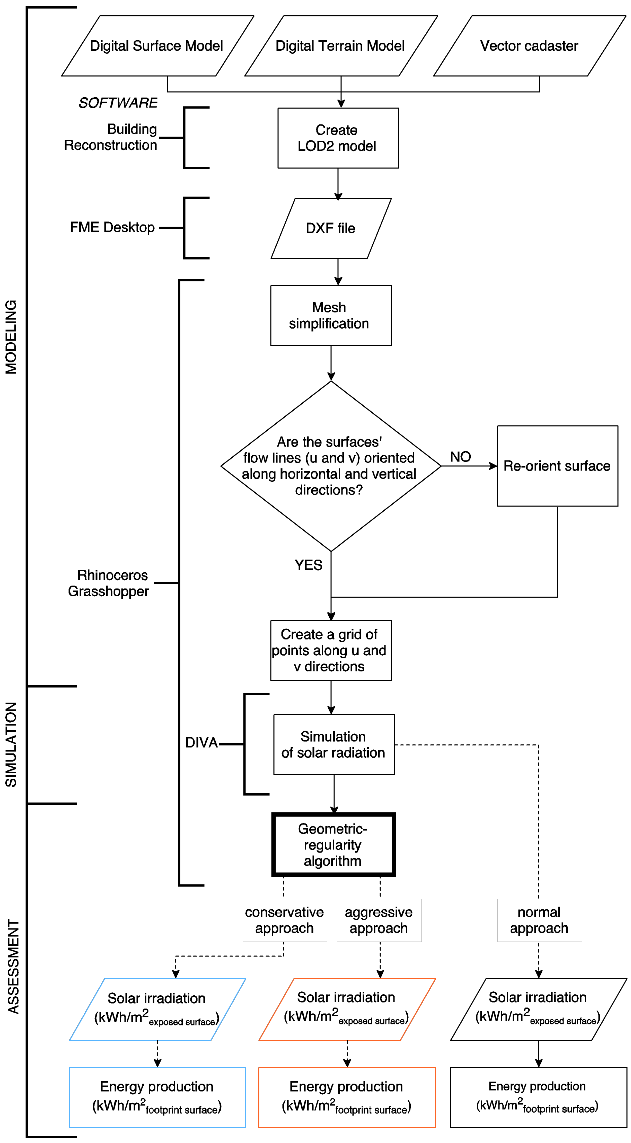

Fig 6 - Flowchart of the modeling, simulation and assessment phases

3.2 Simulation

A weather file for the city of Neuchâtel was created in Meteonorm (Remund, 2014) on the basis of the latest available recorded data (1991-2010). The simulation was run through Diva-for-Grasshopper (Solemma, 2014), a graphical interface to Radiance (Ward, 1994), using the GenCumulativeSky algorithm (Robinson & Stone, 2004), which provides the annual cumulative solar irradiation for each sensor point, expressed in kWh/m^2.

3.3 Assessment

The simulation results were processed through the geometric-regularity algorithm and transformed into energy production, as shown in Fig 6. We used fixed module efficiency coefficients of 15% for roof and of 8% for facades surfaces, considered among the standard values for, respectively, polycrystalline silicon- and cadmium telluride-based modules (Häberlin, 2012, para. 1.4.2). The latter is considered a more suitable technology for facade installation, due to the higher probability of having partial shading on some cells, which would more highly affect the performance of polycrystalline modules (Khaing, Liang, Htay, & Fan, 2014), as well as because of the wide range of possible installations as thin-film (e.g. on shading devices or integrated in glazing).

The irradiation results, expressed in kWh/m^2 of exposed surface, were transformed in kWh by multiplying the value of each point by the sensor point mean area, calculated by dividing the area of each surface s_b by the number of sensor points $p_{b,s,l}$. The obtained values were then converted to energy production using the above-mentioned PV-efficiency coefficients and finally normalized in kWh/m^2 of footprint surface in order to compare buildings of different sizes with the same reference scale.

We conducted thus a sensitivity analysis in order to check the influence of different irradiation thresholds on the energy production calculated with the geometric-regularity algorithm.

Fig 7 and Fig 8 show that the use of the conservative and aggressive approaches determine, respectively, a reduction and an increment in the energy production with respect to the normal calculation method (i.e. the one without geometry sampling) for all selected irradiation thresholds, except for those from 1175 to 1250 kWh/m^2 as no sensor point is within this range (Fig 4 and Fig 5). Moreover, the difference in energy production can vary significantly depending on the chosen threshold and the geometric-regularity approach.

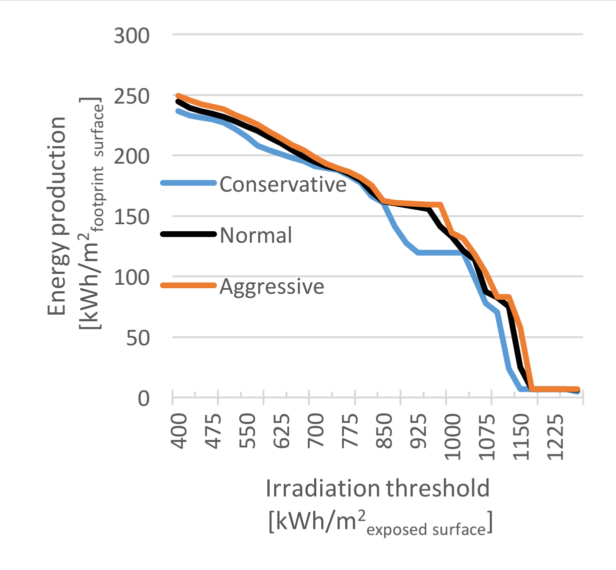

Fig 7: Energy production associated to the proposed approaches

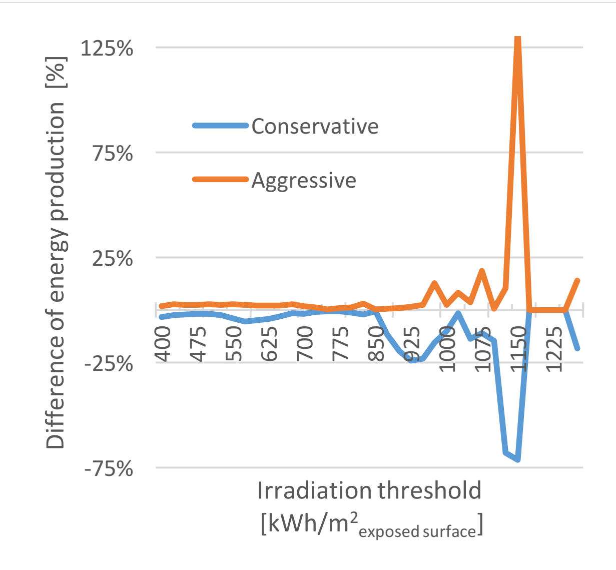

Fig 8: Difference between the normal and the geometry-sampling approaches

In general, the loss in energy production due to the conservative approach is greater than the possible increment due to the aggressive approach. However, this is not the case for a threshold of 1150 kWh/m^2, which brings about a 134% increment for the aggressive approach and only a 71% reduction for the conservative approach. In this case, only scattered roof parts of buildings A and B achieve the irradiation threshold and are hence discarded using the conservative approach, while a much larger surface gets considered if the normal and aggressive approaches are implemented, as can be observed in the fourth column of Fig 9.

4. Limitations and future work

In this work we used a geometry-sampling method to evaluate the BIPV-suitability of building surfaces. However, other criteria should be included such as, for example, the context sensitivity and the system visibility proposed by Munari Probst & Roecker (2011), as well as a more extensive analysis on the architectural features, in terms for example of materials, colors, surface textures and joints (*ibid*.). Moreover, the proposed workflow to select the appropriate BIPV systems should be further developed to identify, for instance, partially shaded zones where the installation of crystalline silicon-based solar cells should be avoided, unless micro-inverters are used in order to prevent the loss in energy production. The efficiency of the cells should then be adjusted according to the actual installation conditions of the solar panels, for example in terms of temperature.

Regarding the software platform, the algorithm relies on Diva-for-Grasshopper as the interface to the simulation engine. We aim at porting it into a platform-independent code so that it can be integrated into other simulation tools (such as Honeybee) or coupled directly with simulation engines such as Radiance or CitySim. Finally, the effectiveness of the proposed method in identifying BIPV-suitable surfaces has to be validated.

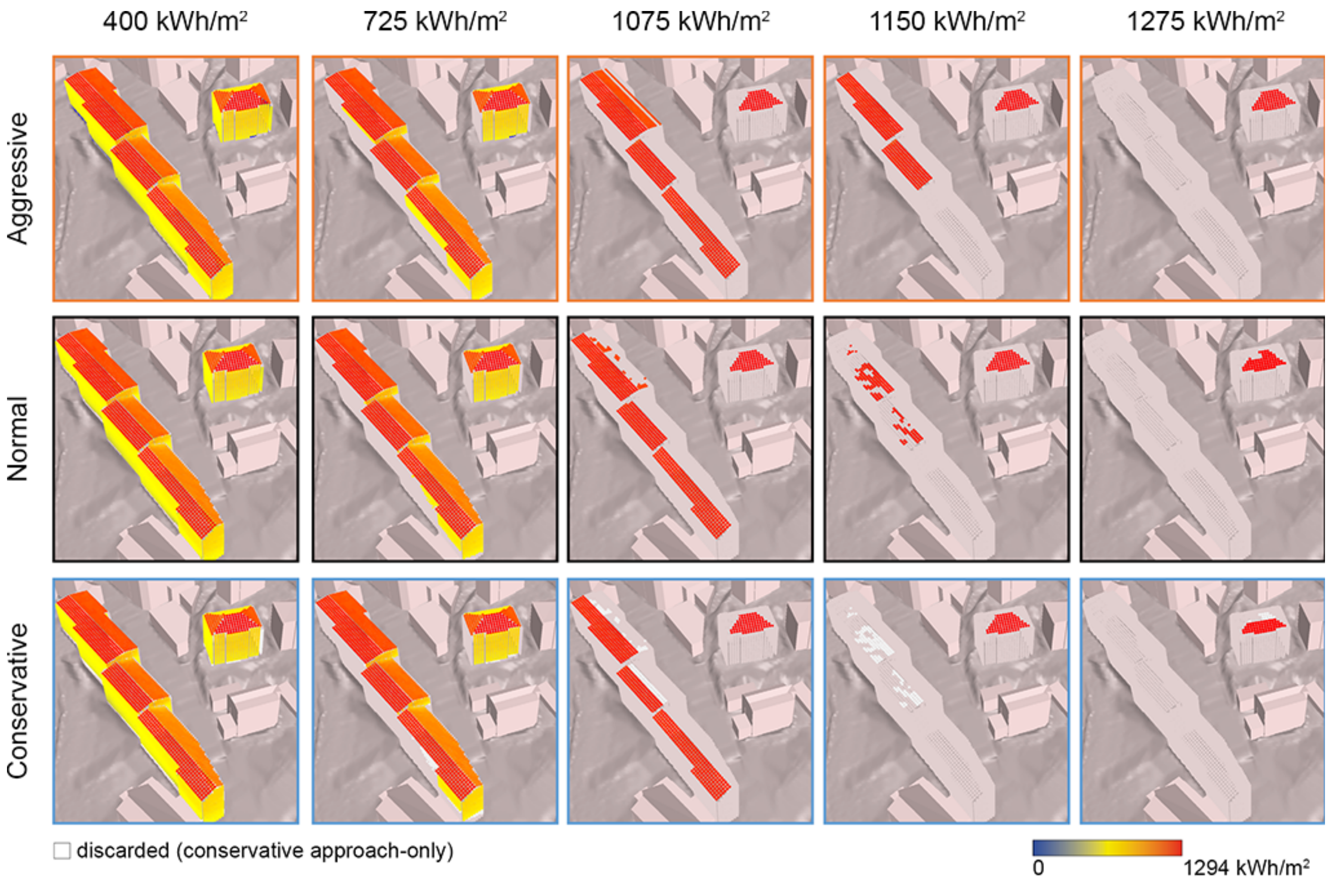

Fig 9: BIPV-suitable surfaces as defined by the proposed approaches for different irradiation thresholds

A first step towards validation will be the comparison of the results obtained with those calculated on an architectural-scale model with a higher level of detail (LOD3) and carefully-designed PV integration.

5. Conclusions

This paper presented the early development of a methodology to assess the BIPV potential in urban contexts in order to inform the planning and the design processes. We proposed an algorithm integrating geometric-regularity criteria in the definition of BIPV-suitable surfaces. We demonstrated its applicability to a LOD2 model produced by high-definition GIS data, which makes possible its use for large urban areas. Although the results cannot be generalized, we showed that the proposed conservative and aggressive approaches can determine energy production values that greatly differ from those calculated through a method based only on an irradiation threshold and that this difference can vary significantly depending on the selected threshold.

The two proposed approaches both respond to the geometric-regularity requirement, even if they represent opposed strategies to deal with such criterion. Although it is difficult to predict which strategy will be chosen in the actual BIPV installation, the proposed methodology is expected to provide helpful guidance when evaluating the solar energy potential in urban environments, as it provides an estimation of the error rate that irradiation threshold-based methods can have if geometric regularity is not considered.

6. Acknowledgements

This work has been conducted as part of the ACTIVE INTERFACES research project (Lufkin, Rey, Wuestenhagen, Wittkopf, & Bacher, 2015), which received financial support from the Swiss National Science Foundation (SNSF) within the framework of the National Research Program NRP 70 "Energy Turnaround". Additional support has been granted by the Ecole polytechnique fédérale de Lausanne (EPFL). The authors would like to thank Dr. Sophie Lufkin, Dr. Luisa Pastore and Emilie Nault for their constructive feedback.

7. References

Compagnon, R. (2004). Solar and daylight availability in the urban fabric. *Energy and Buildings*, *36*(4), 321–328.

Häberlin, H. (2012). *Photovoltaics System Design and Practice*. Chichester, UK: John Wiley & Sons.

Heinstein, P., Ballif, C., & Perret-Aebi, L.-E. (2013). Building Integrated Photovoltaics (BIPV): Review, Potentials, Barriers and Myths. *Green*, *3*(2).

IEA. (2002). *Potential for Building Integrated Photovoltaics - Full Technical Report* (PVPS T7-4).

Jakubiec, J. A., & Reinhart, C. F. (2012). Towards validated urban photovoltaic potential and solar radiation maps based on lidar measurements, GIS data, and hourly daysim simulations. In *Proceedings of SimBuild 2012*. Madison

Kanters, J., Wall, M., & Dubois, M.-C. (2014). Development of a Façade Assessment and Design Tool for Solar Energy (FASSADES). *Buildings*, *4*(1), 43–59.

Khaing, H. H., Liang, Y. J., Htay, N. N. M., & Fan, J. (2014). Characteristics of Different Solar PV Modules under Partial Shading. *International Journal of Electrical, Computer, Electronics and Communication Engineering*, *8*(9), 1333–1337.

Kolbe, T. H., Gröger, G., & Plümer, L. (2005). CityGML: Interoperable Access to 3D City Models. In P. D. P. van Oosterom, D. S. Zlatanova, & E. M. Fendel (Eds.), *Geo-information for Disaster Management* (pp. 883–899). Springer Berlin Heidelberg.

Lufkin, S., Rey, E., Wuestenhagen, R., Wittkopf, S., & Bacher, P. (2015, April 24). *Building integrated photovoltaics | ACTIVE INTERFACES*. Poster presented at the Kick-off meeting of the National Research Programmes NRP 70 "Energy Turnaround" and NRP 71 "Managing Energy Consumption", Luzern.

McNeel. (2014). Grasshopper (Version 0.9.0.76) [Windows]. Seattle, WA, USA: Robert McNeel & Associates.

Munari Probst, M. C., & Roecker, C. (2011). Urban acceptability of building integrated solar systems: Leso QSV approach. In *Proceedings of ISES 2011*. Kassel.

Redweik, P., Catita, C., & Brito, M. (2013). Solar energy potential on roofs and facades in an urban landscape. *Solar Energy*, *97*, 332–341.

Remund, J. (2014). Meteonorm: Irradiation data for every place on Earth (Version 7). Bern: Meteotest.

Robinson, D., & Stone, A. (2004). Irradiation modelling made simple: the cumulative sky approach and its applications. In *Proceedings of PLEA 2004*. Eindhoven.

SFOE. (2014). Energy Strategy 2050. Swiss Federal Office of Energy (SFOE).

SFOE. (2015). Production et Consommation Totales d'Énergie Électrique en Suisse 2014. Swiss Fderal Office of Energy (SFOE).

SMS. (2013). Panneaux solaires: fiche des recommandations. Canton de Genève, Service des monuments et des sites (SMS).

Solemma. (2014). DIVA-for-Grasshopper (Version 3.0.0.6) [Windows]. Cambridge: Solemma.

virtualcitySystems. (2014). BuildingReconstruction (Version 2014.0.1.0) [Windows]. Berlin: virtualcitySystems GmbH.

Ward, G. J. (1994). The RADIANCE lighting simulation and rendering system. In *Proceedings of the 21st annual conference on Computer graphics and interactive techniques* (pp. 459–472). New York: ACM.